Since January 2020 Elsevier has created a COVID-19 resource centre with free information in English and Mandarin on the novel coronavirus COVID-19. The COVID-19 resource centre is hosted on Elsevier Connect, the company's public news and information website.

Available online at www.sciencedirect.com
ScienceDirect
Chinese Journal of Natural Medicines 2021, **19**(6): 473-480
doi: 10.1016/S1875-5364(21)60046-8
Chinese Journal of Natural Medicines

•Research article•

Chemical profiling of Huashi Baidu prescription, an effective anti-COVID-19 TCM formula, by UPLC-Q-TOF/MS

WEI Wen-Long[Δ], WU Shi-Fei[Δ], LI Hao-Jv, LI Zhen-Wei, QU Hua, YAO Chang-Liang, ZHANG Jian-Qing, LI Jia-Yuan, WU Wan-Ying, GUO De-An[*]

Shanghai Research Center for Modernization of Traditional Chinese Medicine, National Engineering Laboratory for TCM Standardization Technology, Shanghai Institute of Materia Medica, Chinese Academy of Sciences, Shanghai 201203, China

Available online 20 Jun., 2021

[ABSTRACT] Huashi Baidu prescription (HSBDF), recommended in the Guideline for the Diagnosis and Treatment of Novel Coronavirus (2019-nCoV) Pneumonia (On Trials, the Seventh Edition), was clinically used to treat severe corona virus disease 2019 (COVID-19) with cough, blood-stained sputum, inhibited defecation, red tongue etc. symptoms. This study was aimed to elucidate and profile the knowledge on its chemical constituents and the potential anti-inflammatory effect *in vitro*. In the study, the chemical constituents in extract of HSBDF were characterized by UPLC-Q-TOF/MS in both negative and positive modes, and the pro-inflammatory cytokines were measured by enzyme-linked immunosorbent assays (ELISA) to determine the effects of HSBDF in lipopolysaccharide (LPS)-stimulated RAW264.7 cells. The results showed that a total of 217 chemical constituents were tentatively characterized in HSBDF. Moreover, HSBDF could alleviate the expression levels of IL-6 and TNF-α in the cell models, indicating that the antiviral effects of HSBDF might be associated with regulation of the inflammatory cytokines production in RAW264.7 cells. We hope that the results could be served as the basic data for further study of HSBDF on anti-COVID-19 effect.

[KEY WORDS] Huashi Baidu prescription; Corona virus disease 2019; Characterization of chemical constituents; ELISA
[CLC Number] R917 **[Document code]** A **[Article ID]** 2095-6975(2021)06-0473-08

Introduction

Corona Virus Disease 2019 (COVID-19), a highly pathogenic Human coronaviruses (hCoVs), could cause viral pneumonia and pulmonary infection. COVID-19 possessed long latency, strong infectivity and difficult to cure features etc., which threaten the people's health, economic development and social harmony [1]. By October 21, 2020, more than 40 000 000 people have been firmly diagnosed with COVID-19 around the world according to the statistical information of 1point3acres (https://coronavirus.1point3acres.com/), and there has been still no effective drugs to cure the devastating disease. According to the ancient Chinese documents and clinical experience, traditional Chinese medicine (TCM) had a good curative effect on viral pneumonia. National health and health commission (PRC) have updated and released in the Guideline for the Diagnosis and Treatment of Novel Coronavirus (2019-nCoV) Pneumonia (On Trials, the Seventh Edition), and the TCMs were recommended for prevention and treatment of COVID-19. In the Seventh Edition, Huashi Baidu Fang (HSBDF) consists of 14 hebal medicines (Ephedrae herba, Armeniacae semen amarum, Gypsum fibrosum, Glycyrrhizae radix et rhizoma, Agastache rugosus, Magnoliae officinalis cortex, Atractylodis rhizoma, Tsaoko fructus, Pinelliae rhizoma praeparatum, Poria, Rhei radix et rhizoma, Astragali radix, Descurainiae semen lepidii semen, Paeoniae radix rubra) were recommended and used to treat the critical patients with COVID-19 infection, and exhibited good therapeutic effect in clinical practice [2]. HSBDF was developed referred to multiple classical prescriptions (Ma Xing Shi Gan Decoction, Xuan Bai Cheng Qi Decoction, Dayuanyin, Huoxiangzhengqqi San, Taoren Chengqi Decoction, Tingli Dazao Xiefei Decoction) for treatment of fever, cough, nausea, etc. Ma Xing Shi Gan Decoction and Xuan Bai Cheng Qi Decoction mainly used for facilitaing lung and

[Received on] 30-Oct.-2020
[Research funding] This work was supported by the National Key R&D Program of China (2019YFC1711000), Qi-Huang Scholar of National Traditional Chinese Medicine Leading Talents Support Program (2018), Chief Scientist of Qi-Huang Project of National Traditional Chinese Medicine Inheritance and Innovation "One Hundred Million" Talent Project (2020).
[*Corresponding author] Tel: 86-21-20231000-2211, Fax: 86-21-50272789, E-mail: gda5958@163.com
[Δ]These authors contributed equally to this work.
These authors have no conflict of interest to declare.

clearing excretion, evacuating upper-jiao [3-4]. Dayuanyin and Huoxiangzhengqqi San were used for dissipating hygrosis restore stomach, mediating middle-jiao [5-6]. Taoren Chengqi Decoction, Tingli Dazao Xiefei Decoction were applied for treating cardiac failure and eliminating toxicant, reaching lower-jiao [7-8]. Among them, Ma Xing Shi Gan Decoction has been clinically applied to treat Coronavirus Disease 2019 with fever, weakness and cough [9-11].

However, the detailed analysis involved in the chemical components, the comprehensive mechanisms and the active ingredients responsible for antiviral effectiveness of HSBD remained elusive. TCM prescription was a complex system, and the efficient detection and characterization of the potentially bioactive compounds in TCM prescriptions was still a massive challenge. Recently, ultra-high performance liquid chromatography coupled with high resolution mass spectrometry (LC-HRMS) has proved its superiority in structural profiling of complex components [12]. On the one hand, LC-HRMS was able to offer the potential chemical element composition and infer the detailed structure of analytes on the basis of the measurement of accurate mass and generation of the MS/MS or MS^n data [13]. On the other hand, due to the advantages of high-efficiency, high-throughput screening and low solvent consumption, it could determine hundreds or even thousands of MS features using a single injection in a short time and with less consumption of organic solvents [14]. LC-HRMS has been used for comprehensive characterization of chemical constituent of anti-COVID-19 TCM formulas, such as qingfei paidu decoction, maxing shigan decoction and lianhuaqingwen capsule [15-17]. Enzyme-linked immunosorbent assay (ELISA) was a sensitive immunoassay that used an enzyme linked to an antibody or antigen as a marker for the detection of a specific protein. It was usually applied for the quantification of diverse pathological factors due to its convenient, fast and accurate advantages in the determination of a series of inflammatory cytokines in many suitable situations.

With the unraveling of the relationship between immune responses and COVID-19, immune characteristics are now being recognized as potential biomarkers for disease progression as well as potential therapeutic targets for COVID-19 [18-21]. In the present study, a UPLC-Q-TOF/MS method was developed for rapid characterization of chemical constituents in HSBDF. Then, lipopolysaccharide was subsequently used to simulate the inflammatory response in the RAW64.7 cells to explore the potential anti-inflammation effect of HSBD. High concentrations of cytokines were also recorded in plasma of patients infected with COVID-19 in Wuhan, such as GCSF (granulocyte macrophage-colony stimulating factor), IL-6 (interlukin-6), IL-1β (interleukin 1beta)and TNF-α (tumor necrosis factor-alpha), suggesting that the cytokine storm was associated with disease severity in COVID-19 infection. To determine the effect of HSBDF on the regulations of the related pro-inflammatory cytokines, the expression levels of IL-6 and TNF-α in the cell supernatant were measured by ELISA. The data suggested that the anti-virus activity of HSBDF might be associated with an attenuated proinflammatory cytokine response.

Experimental

Materials and reagents

HPLC-grade acetonitrile and methanol were purchased from Merck KGaA (Merck, Darmstadt, Gemany). Formic acid (FA) was purchased from Sigma-Aldrich (Sigma-Aldrich, StLouis, MO, USA), and deionized water (18.2 MΩ·cm at 25 °C) was prepared by a Millipore Alpha-Q water purification system (Millipore, Bedford, USA). The herbal materials of ephedrae herba (voucher specimen number: EH20200601), armeniacae semen amarum (ASA20200601), gypsum fibrosum (GF20200601), glycyrrhizae radix et rhizoma (GA20200601), agastache rugosus (ARU20200601), magnoliae officinalis cortex (MOC20200601), atractylodis rhizoma (ARH20200601), tsaoko fructus (TF20200601), pinelliae rhizoma praeparatum (PRP20200601), poria (P20200601), rhei radix et rhizoma (RRR20200601), astragali radix (ARA20200601), descurainiae semen lepidii semen (DSLS20200601), paeoniae radix rubra (PRR20200601) were purchased from Shanghai Dehua National Pharmaceutical Products Co. Ltd. (Shanghai, China), Shanghai Huaying Pharmaceutical Co. Ltd. (Shanghai, China), Shanghai Qingpu Traditional Chinese Medicine Yinpian Co. Ltd. (Shanghai, China), Shanghai Yutiancheng Traditional Chinese Medicine Yinpian Co. Ltd. (Shanghai, China). All the herbal materials were authenticated by Professor GUO De-An following the method described in China Pharmacopeia (2015 edition), and the voucher specimens were deposited at the authors' lab in Shanghai Institute of Materia Medica, Chinese Academy of Sciences (Shanghai, China). Eight reference standards (ephedrine, pseudoephedrine, liquiritin, glycyrrhizic acid, aloe-emodin, rhein, physcion, quercetin-3-*O*-*β*-D-glucose-7-*O*-*β*-gentiobioside) were purchased from National Institutes for Food and Drug Control (Beijing, China), Six reference standards (calycosin-7-*O*-*β*-D-glucoside, magnolol, honokiol, amygdalin, emodin, astragaloside IV) were purchased from Shanghai Nature Standard Technical Service Co., Ltd. (Shanghai, China), Paeoniflorin was purchased from Sichuan Weikeqi Biological Technology Co., Ltd. (Sichuan, China). The Purity of all reference standards was more than 98%.

The extracted liquid of HSBDF for cell treatment was obtained as described above, which was finally adjusted to 10 μg·μL^{-1} with phosphate buffered saline (PBS) filtered through a 0.22 μm syringe filter, and stored at −20 °C until use. Lipopolysaccharides (LPS, from *Escherichia coli* serotype 055: B5) were purchased from Sigma-Aldrich (St. Louis, MO, USA). 3-(4, 5-Dimethylthiazol-2-yl)-2, 5-diphenyltetrazolium bromide (MTT), dimethylsulfoxide (DMSO) were obtained from Millipore (Billerica, MA, USA). Dulbecco's modified Eagle's medium (DMEM) and fetal bovine serum (FBS) were purchased from Gibco (Grand Island, NY, USA).

The ELISA kits for IFN-β, IL-6 and TNF-α were purchased from the Boster Bioengineering Institute (Shanghai, China).

Sample preparation

Sample preparation for characterization of chemical constituents in HSBDF: an amount of herbal materials was accurately weighed according to the prescription dose. The herbal materials (ephedrae herba, armeniacae semen amarum, gypsum fibrosum, glycyrrhizae radix et rhizoma, magnoliae officinalis cortex, atractylodis rhizoma, tsaoko fructus, pinelliae rhizoma praeparatum, poria, astragali radix, descurainiae semen lepidii semen, paeoniae radix rubra) were added into gallipot, and soaked for 10 minutes with ten times the amount of water. Then the herbal materials (agastache rugosus and rhei radix et rhizoma) were added when the water began to boil slightly. The prescription was decocted twice, and each time for 30 min. The extract was merged and dried by freeze drying. The 0.1 g HSBDF freeze dried sample was weighed and added 10 mL methanol−water (1 : 1, *V*/*V*) to prepare test solution, the supernatant was centrifuged at 14 000 r·min^{-1} before LC-MS analysis.

UPLC-Q-TOF/MS analysis conditions

Chromatographic separation of HSBDF was performed on a Waters ACQUITY I-Class UPLC® system (Waters Corporation, Milford, MA, USA) equipped with an ACQUITY UPLC® HSS T3 column (1.8 μm, 2.1 mm × 100 mm). The HSBDF was eluted by a binary mobile phase composed of acetonitrile (B) and 0.1% formic acid (*V*/*V*; A) following the gradient elution program: 0−20 min: 0−60% B; 20−22 min: 60%−90% B; 22−25 min: 90%−90% B. The flow rate was 0.3 mL·min^{-1}, the column temperature was set at 30 °C, and 5 μL of the test solution was injected for analysis.

High-resolution profile MS data were acquired on a Waters Xevo® G2-S QTOF mass spectrometer (Waters, Manchester, UK) connected to the UPLC system *via* a Zpray™ ESI source. The mass range of *m*/*z* 150−1500 was set for full-scan, and the collision energy ramp of 15−25 V and 35−45 V were set for low mass and high mass, respectively. Capillary voltages of 2 kV, cone voltage of 40 V, cone gas flow of 30 L·h^{-1}, source temperature of 140 °C, and desolvation gas flow of 700 L·h^{-1} at 500 °C were utilized. A solution of leucine-enkephalin (1 μg·mL^{-1}) was used as lock mass for data calibration.

Cell culture

Murine macrophage cell line (RAW264.7) was purchased from the Type Culture Collection of the Chinese Academy of Sciences, Shanghai, China. RAW264.7 cells were cultured in DMEM supplemented with 10% FBS and antibiotics (100 U·mL^{-1} penicillin G and 100 μg·mL^{-1} streptomycin) (Gibco). Cells were cultured under standard condition (5 % CO_2 in air in a humidified environment at 37 °C).

Cytotoxicity assay

RAW264.7 cells were placed in 96-well plates at a density of 4 × 10^4 cells/mL for 24 h and then treated with different concentrations of HSBDF. Cell viability was measured by the MTT assay method according to the instructions. The absorbance was measured at 490 nm with a microplate reader (Thermo Scientific Varioskan LUX). The normal control (cells with no treatment) was set at 100%, and the treated samples were normalized to this value. The 50% cytotoxic concentration (CC_{50}) was calculated as the concentration of HSBDF causing the death of 50% of the cells.

Determination of inflammatory cytokines by enzyme-linked immunosorbent assay (ELISA)

The cells were seeded in 12-well plates (3 × 10^5 cells/well) and were co-treated with HSBDF (20 and 100 μg·mL^{-1}) in the presence of LPS (1 μg·mL^{-1})(except for the Blank group) for 4 or 12 h. After centrifugation, cell-free supernatants were collected for assaying TNF-α, IL-6 production. The secretion amount of TNF-α, IL-6 in the media were measured through ELISA kits (Boster, Shanghai, China) by following the standard protocol. The 450 nm absorbance was tested through a microplate reader (Thermo Scientific Varioskan LUX).cientific Varioskan LUX).

Data processing

MassLynx V4.1 software (Waters, Milford, USA) was employed in data acquisition and processing. One-way analysis of variance (ANOVA) and Student's *t*-test were used to assess differences between the treatment groups. The *P* values less than 0.05 were considered as statistically significant. The CC_{50} values were calculated by nonlinear regression in GraphPad Prism 5 (San Diego, CA, USA).

Results and Discussion

Optimization of LC and MS conditions

In order to acquire good separation and peak shapes, the mobile phase system (methanol−water/acetonitrile−water), type of column (BEH C18, HSS T3 and BEH HILIC), column temperature (30, 35, 40 °C) were optimized. The 0.1% formic acid water−acetonitrile were selected as mobile phase system to obtain good distribution for the majority of peaks, HSS T3 column possessed better separation capacity among three different columns, and the column temperature was set 30 °C.

For the MS conditions, both the positive and negative mode were applied for characterization of chemical constituents in HSBDF due to the abundant MS information (Fig. 1). Meanwhile, the capillary voltage, cone voltage and collision energy were optimized, and 2 kV for capillary voltages, 40 V for cone voltage, 15–25 V and 35–45 V were set for collision energy ramp of low mass and high mass.

Characterization of chemical components in HSBDF extract

An UPLC-Q-TOF/MS method was developed for comprehensive characterization of chemical constituents in HSBDF extract in both negative and positive mode. A total of 217 chemical constituents including (alkaloid, flavone, terpenoid, lactones, lignan, phenylpropanoids, phenolic acid, saponin, anthraquinone, others) were tentatively identified based on the MS information, fragmentation pattern of standards and published references, among which 69 chemical constituents were identified in positive mode, and 148 chem-

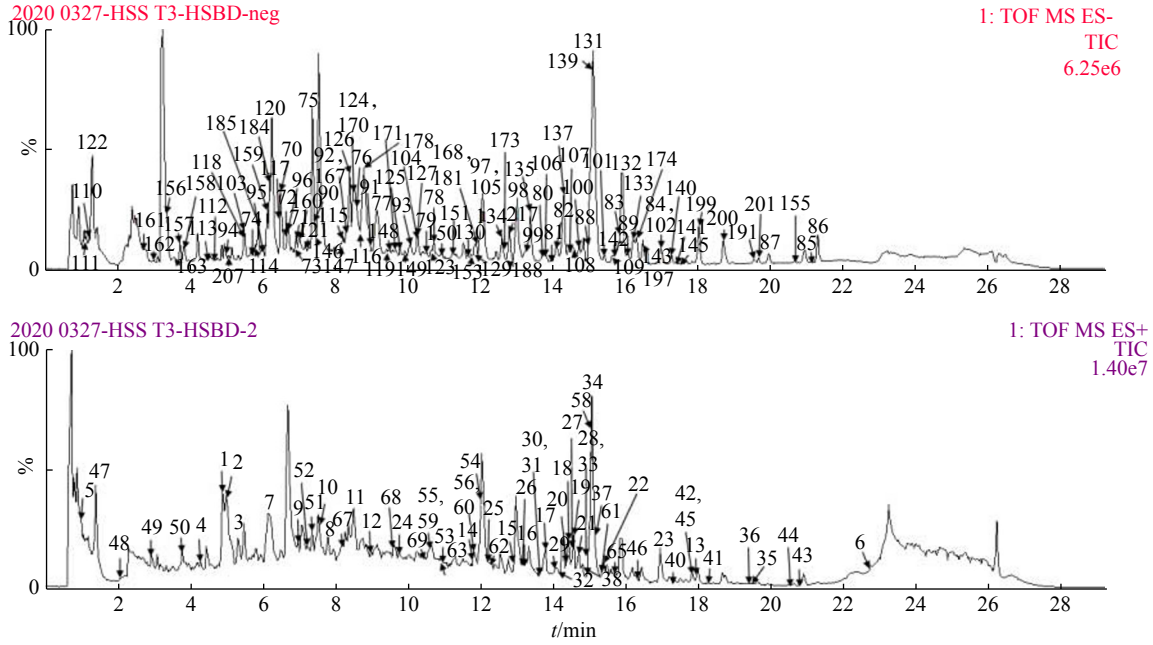

Fig. 1 Characterization of chemical constituents in HSBDF. The chemical constituents in HSBDF extract were characterized in both negative and positive mode by UPLC-Q-TOF/MS

ical constituents were identified in negative mode (Fig. 2). Among them, 14 chemical constituents were identified through comparing the retention time and MS spectra of standards. The numbers of flavone and saponin compounds were higher than other compounds, and accounted for 36% and 10% respectively (Fig. 3).

Components from ephedrae herba

Alkaloids were the main bioactive constituents in ephedrae herba, and possessed good therapeutic effect with asthma [22]. Alkaloids had better abundance in positive mode, and the main adduct form was $[M + H]^+$ peak. Take ephedrine as an example, ephedrine showed an $[M + H]^+$ ion at *m/z* 166.12, and fragmented into three products at *m/z* 148.11, 133.08, 117.06 (Fig. 4). As shown in Fig. 4c, ephedrine generated bond fission of hydroxyl with loss a H_2O (18 Da), then dehydroxylated-ephedrine was further fragmented to the product ion at *m/z* 133 and 117 through losing a CH_3 or NH_2-CH_3 [23]. Thus, four alkaloids from ephedrae herba were identified. Meanwhile, proline and diisobutyl phthalate were also

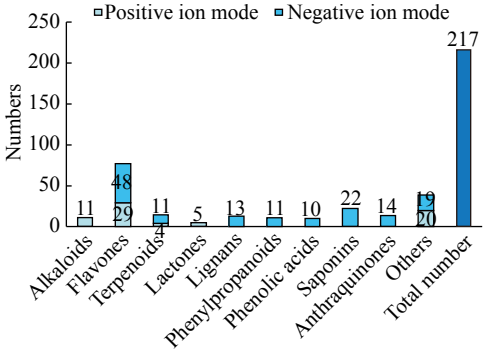

Fig. 2 Diversity of chemical constituents in HSBDF

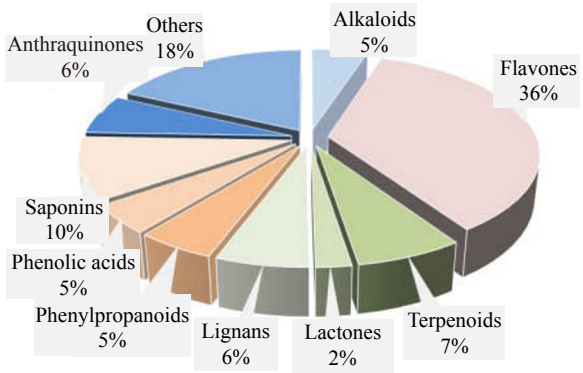

Fig. 3 Proportion of different types of chemical constituents in HSBDF

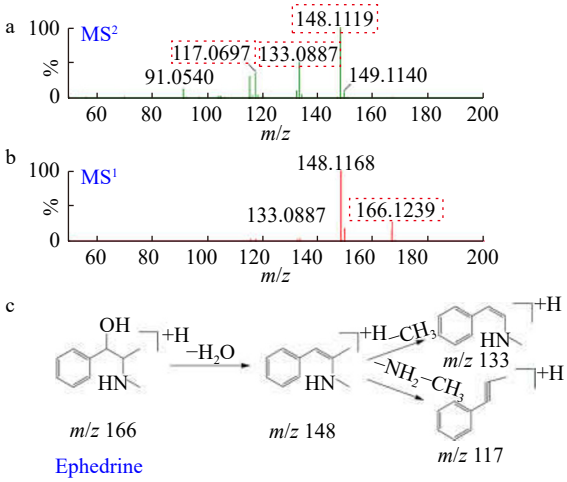

Fig. 4 Deduction of fragmentation pattern of ephedrine. Ephedrine showed an $[M + H]^+$ ion at *m/z* 166.12, and fragmented into three products at *m/z* 148.11, 133.08, 117.06

detected [24, 25].

Components from astragali radix

There were 13 flavone, 3 other compounds and 9 saponin were supposedly identified in both positive and negative ion mode from astragali radix [26]. In the positive ion mode, flavone compounds exhibited the $[M + H]^+$ ion form, calycosin-7-*O*-*β*-D-glucoside was used as a case for deduction of fragmentation pattern (Fig. S1). The precursor ion of calycosin-7-*O*-*β*-D-glucoside (*m*/*z* 447.1277) was observed at 8.32 min, and fragmented into *m*/*z* 285 by losing a glucose ($C_6H_{10}O_5$). The fragment (*m*/*z* 285) was further produced three product ions (*m*/*z* 270, 253 and 137) with loss of CH_3, CH_3O and $C_9H_7O_2$ (Fig. S1d). The saponin compounds possessed good response in negative ion mode, and represented $[M + COOH]^-$ ion form. The fragmentation pattern was showed with astragaloside IV. The precursor ion (*m*/*z* 829.4582) was observed at 14.52 min in MS1 and translated into $[M - H]^-$ ion form in MS2 (Fig. S2). Meanwhile, the C-3 and C-6 position C-O bonds of $[M - H]^-$ ion were broken and generated two characteristic fragments (*m*/*z* 621 and *m*/*z* 489). The fragment (glucose, *m*/*z* 179) was further ruptured and produced *m*/*z* 161, 119 and 101 (Fig. S2c) d 101 (Fig. S2c) [27]. According to the fragmentation pattern and published references, 9 saponin compounds from astragali radix were tentatively identified in HSBDF [28-29].

Components from magnoliae officinalis cortex

There were 7 alkaloids, 2 flavones, 3 phenylpropanoids, 12 lignans and 6 other compounds identified from magnoliae officinalis cortex in positive and negative ion mode [30-31]. For the identification of lignans, magnolol and honokiol were used to deduce the fragmentation pattern (Fig. S3). In negative ion mode, magnolol and honokiol presented $[M - H]^-$ ion form (*m*/*z* 265 and 265), and the main characteristic fragments were *m*/*z* 247 and 224 with loss of OH and C_3H_5 [32]. Furthermore, 7 alkaloids were supposedly identified on the basis of the published references [33-34].

Components from armeniacae semen amarum and glycyrrhizae radix et rhizoma

Two compounds (amygdalin and prunasin) were identified from xingren. The MS1, MS2 and fragmentation pattern of amygdalin were shown in Fig. S4. A total of 20 flavones, 13 saponins, 1 disaccharide and 1 phenylpropanoids were found from gancao. One flavone (liquiritin) and saponin (glycyrrhizic acid) were applied for deduction of fragmentation pattern. For the liquiritin, the glycoside was lost from $[M - H]^-$ ion (*m*/*z* 417) and the *m*/*z* 255 was further fragmented into *m*/*z* 135 and 119 (Fig. S5). For the saponin, the precursor ion was $[M - H]^-$ ion at *m*/*z* 821, and the main fragment ions (*m*/*z* 645 $[M - H\text{-}(C_6H_8O_6)]^-$, *m*/*z* 351 $[2C_6H_8O_6 - H]^-$, *m*/*z* 193 $[C_6H_9O_7]^-$) that were generated *via* the MS/MS fragmentation were observed in the negative ion spectrum [35].

Components from rhei radix et rhizoma

Forty compounds including 7 phenolic acids, 7 flavones, 14 anthraquinones, 3 phenylpropanoids and 8 other compounds from rhei radix et rhizoma were tentatively identified in negative ion mode [36-37]. For the anthraquinones, emodin and rhein were used as examples to illustrate the characterization process. The characteristic fragments (*m*/*z* 241 and 225) were fractured from $[M - H]^-$ ion (emodin) at *m*/*z* 821 by losing CO and OH (Fig. S6). The $[M - H]^-$ ion of rhein was presented at *m*/*z* 283 in MS1, and the fragments (*m*/*z* 239, 211 and 183) were produced with loss of COOH, CO and CO in MS2 (Fig. S7). The phenolic acids, flavones and phenylpropanoids were supposedly characterized through comparing with elementary composition and characteristic fragments derived from published references [38-39].

Components from descurainiae semen lepidii semen

There were 6 flavones from descurainiae semen lepidii semen were tentatively identified under negative ion mode in HSBDF [40-41]. Quercetin-3-*O*-*β*-D-glucose-7-*O*-*β*-gentiobioside showed $[M - H]^-$ form at *m*/*z* 787, and three fragments (*m*/*z* 625 $[M - H\text{-glc}]^-$, *m*/*z* 463 $[M - H\text{-2glc}]^-$, and *m*/*z* 301 $[M - H\text{-3glc}]^-$) were observed in MS2 (Fig. S8). The fragmentation pattern of quercetin-3-*O*-*β*-D-glucose-7-*O*-*β*-gentiobioside was exhibited in Fig. S8c.

Components from paeoniae radix rubra

A total of 14 components (2 phenolic acids, 2 flavones and 11 terpenoids) from paeoniae radix rubra were tentatively identified in HSBDF [32-43]. Paeoniflorin was used as a case for elucidation of proposed fragmentation pathways of terpenoids. As shown in Fig. S9, the precursor ion was $[M + COOH]^-$ form at *m*/*z* 525 in MS1, and three fragments (*m*/*z* 449, 327 and 121) were produced in MS2. The *m*/*z* 449 was generated by losing a HCHO (30Da), and further fragmented into a minor fragment ion at *m*/*z* 327 and a benzoic acid ($[M - H]^-$, 121 Da). According to the fragmentation pattern, 11 terpenoids were tentatively characterized in HSBDF [44-47].

Components from agastache rugosus, atractylodis rhizoma, tsaoko fructusand pinelliae rhizoma praeparatum

There were 17 compounds (1 lignan, 4 phenylpropanoids and 12 flavones) fromagastache rugosus [48-52], 26 compounds (4 terpenoids, 3 flavones, 5 lactones, 1 phenylpropanoid and 13 other compounds) from atractylodis rhizoma [53], 8 compounds (3 phenolic acids and 5 flavones) from tsaoko fructus [54], 8 compounds (4 flavone and 4 other compounds) from pinelliae rhizoma praeparatum were supposedly identified in HSBDF [55-56].

Cytotoxicity assay in RAW264.7 cells

We evaluated cell viability of RAW264.7 cells cultured with different concentrations of HSBDF using the MTT assay to find a suitable concentration for application in the subsequent experiment. These results indicated that the HSBD showed unapparent cytotoxicity to RAW264.7 cells at concentrations up to 200 μg·mL^{-1}. The CC_{50} of HSBDF toward RAW264.7 cells was 417 μg·mL^{-1} (Fig. 5).

Inhibition of the production of TNF-α and IL-6 in LPS-induced RAW 264.7 macrophages

Severe acute respiratory syndrome CoV (SARS-CoV) and Middle East respiratory syndrome CoV (MERS-CoV) were often associated with massive inflammatory cell infiltration and elevated proinflammatory cytokine/chemokine responses resulting in severe respiratory illness. To determine the effect of HSBDF on the expression of proinflammatory cytokine, an *in vitro* LPS-stimulated inflammatory response cell model was established. The expression levels of IL-6 and TNF-α in the cell supernatant were measured by ELISA. As shown in Fig. 6, the elevated expressions of these cytokines induced by LPS in RAW264.7 cells were inhibited by HSBDF treatment in a concentration-dependent manner ($^{*}P < 0.05$).

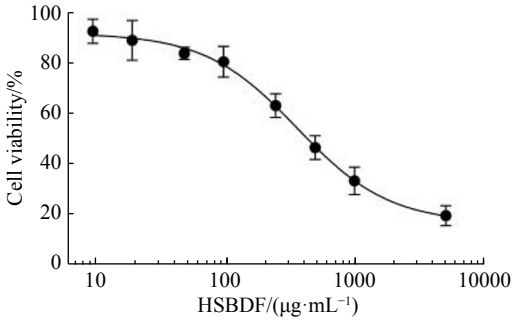

Fig. 5 Cytotoxicity effects of HSBDF. Cell cytotoxicity was detected by a MTT assay according to the manufacturer's instructions. Various concentrations of HSBDF were treated to the cells for 24 h. Data are presented as mean ± SD ($n = 3$)

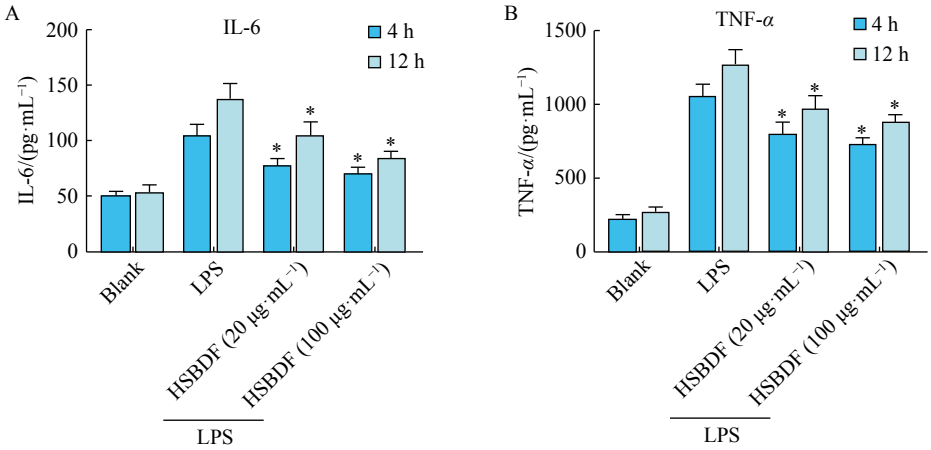

Fig. 6 Effects of HSBDF treatment on the expression levels of inflammatory cytokine in LPS-stimulated RAW264.7 cells *via* ELISA test. (A) IL-6; (B) TNF-α. Data are presented as mean ± SD ($n = 3$), $^{*}P < 0.05$ *vs* blank group

Conclusion

In this study, a rapid method was developed and applied to characterize and profile the chemical components in HSBDF using UPLC-Q-TOF/MS. A total of 217 constituents including alkaloids, flavones, terpenoids, lactones, lignans, phenylpropanoids, phenolic acids, saponins, anthraquinones and other compounds were identified or tentatively characterized. It was known that COVID-19 infection could induce immediate and late host immune responses in patients. Most severe COVID-19 cases exhibited an extreme increase in inflammatory cytokines, including IL-1β, IL-6, IL-10, IFN-γ, and TNF-α, representing a "cytokine storm". Though the precise mechanism of antigen presentation, cellular and humoral immune responses, and cytokine storm during the COVID-19 infection were not yet clearly understood, but the increasing level of IL-6 in COVID-19 patients could induce the differentiation of proinflammatory Th17 cells, upregulate cytokine storm, lung inflammation and dysfunction [57-58]. Thus proinflammatory cytokine expression levels (IL-6 and TNF-α) upon LPS administration in RAW264.7 cells were measured and results were shown that HSBDF could alleviate the expression levels of IL-6 and TNF-α in the cell models, indicating that the antiviral effects of HSBDF might be attributed to the regulation of the inflammatory cytokines production. It is hoped that the results could provide the essential data for the further study on pharmacodynamic material basis of HSBDF in COVID-19.

Supplementary Materials

Supplementary materials are available as Supporting Information, and can be requested by sending E-mail to the corresponding author.

References

[1] Hu Y, Sun J, Dai Z, *et al*. Prevalence and severity of corona virus disease 2019 (COVID-19): a systematic review and meta-analysis [J]. *J Clin Virol*, 2020, **127**: 104371.

[2] Zou BL, Li M, Fan TB, *et al*. Summary of experience and suggestions for TCM treatment of severe COVID-19 [J]. *J Tradit Chin Med*, 2020, **61**(15): 1289-1293.

[3] Wang Y, Zhao B, Fei Y, *et al*. Ma xing shi gan decoction eliminates PM2.5-induced lung injury by reducing pulmonary cell apoptosis through Akt/mTOR/p70S6K pathway in rats [J]. *Biosci Rep*, 2020, **40**(7): BSR20193738.

[4] Qin H, Wen HT, Gu KJ, *et al*. Total extract of Xin Jia Xuan Bai

Cheng Qi decoction inhibits pulmonary fibrosis *via* the TGF-*β*/Smad signaling pathways *in vivo* and *in vitro* [J]. *Drug Des Devel Ther*, 2019, **13**: 2873-2886.

[5] Ruan X, Du P, Zhao K, *et al*. Mechanism of Dayuanyin in the treatment of coronavirus disease 2019 based on network pharmacology and molecular docking [J]. *Chin Med*, 2020, **15**: 62.

[6] Wang, Z, Yang, Z, Grinchuk V, *et al*. Anti-inflammatory and intestinal function-modulating activities of a traditional chinese herbal formula Houxiang Zhengqi [J]. *Gastroenterology*, 2012, **142**(5): S-726.

[7] Fan X, Zhong B, Chen X, *et al*. Experimental study of Taoren Chengqi Decoction on lung injury caused by paraquat poisoning [J]. *JETCM*, 2020, **29**(3): 434-436, 459.

[8] Cheng J, Zeng C, Fang Z. Observation on curative effect of modified Tingli Dazao Xiefei Decoction in treating heart failure [J]. *J Sichuan Tradit Med*, 2020, **38**(6): 96-98.

[9] Yang RC, Liu H, Bai C, *et al*. Chemical composition and pharmacological mechanism of Qingfei Paidu Decoction and Ma Xing Shi Gan Decoction against Coronavirus disease 2019 (COVID-19): in silico and experimental study [J]. *Pharmacol Res*, 2020, **157**: 104820.

[10] Zhang Y, Xu QH, Sun ZY, *et al*. Current targeted therapeutics against COVID-19: based on first-line experience in China [J]. *Pharmacol Res*, 2020, **157**: 104854.

[11] Qu YF, Fang W, Jin YZ, *et al*. Forty Cases of Common COVID-19 Treated with modified ephedra and apricot kernel and gypsum and licorice Decoction combined with western medicine routine treatment [J]. *Henan Tradit Chin Med*, 2020, **40**(5): 666-669.

[12] Yang W, Zhang J, Yao C, *et al*. Method development and application of offline two-dimensional liquid chromatography/quadrupole time-of-flight mass spectrometry-fast data directed analysis for comprehensive characterization of the saponins from Xueshuantong Injection [J]. *J Pharm Biomed Anal*, 2016, **128**: 322-332.

[13] Cui Y, Yang H, Jing J, *et al*. Rapid characterization of chemical constituents of Gansuibanxia decoction by UHPLC-FT-ICR-MS analysis [J]. *J Pharm Biomed Anal*, 2020, **179**: 113029.

[14] Mu X, Xu X, Guo X, *et al*. Identification and characterization of chemical constituents in Dengzhan Shengmai Capsule and their metabolites in rat plasma by ultra-performance liquid chromatography coupled with quadrupole time-of-flight mass spectrometry [J]. *J Chromatogr B Analyt Technol Biomed Life Sci*, 2019, **1108**: 54-64.

[15] Yao CL, Qian ZM, Tian WS, *et al*. Profiling and identification of aqueous extract of *Cordyceps sinensis* by ultra-high performance liquid chromatography tandem quadrupole-orbitrap mass spectrometry [J]. *Chin J Nat Med*, 2019, **17**(8): 631-640.

[16] Zhang ZJ, Wu WY, Hou JJ, *et al*. Active constituents and mechanisms of Respiratory Detox Shot, a traditional Chinese medicine prescription, for COVID-19 control and prevention: Network-molecular docking-LC-MS^{E} analysis [J]. *J Integr Med*, 2020, **18**(3): 229-241.

[17] Chen XF, Wu L, Chen C, *et al*. Identifying potential anti-COVID-19 pharmacological components of traditional Chinese medicine Lianhuaqingwen capsule based on human exposure and ACE_2 biochromatography screening [J]. *Acta Pharm Sin B*, 2021, **11**(1): 222-236.

[18] Kempuraj D, Selvakumar GP, Ahmed ME, *et al*. COVID-19, mast cells, cytokine storm, psychological stress, and neuroinflammation [J]. *Neuroscientist*, 2020, **26**(5-6): 402-414.

[19] Bellinvia S, Edwards CJ, Schisano M, *et al*. The unleashing of the immune system in COVID-19 and sepsis: the calm before the storm? [J]. *Inflamm Res*, 2020, **69**(8): 757-763.

[20] Gao YM, Xu G, Wang B, *et al*. Cytokine storm syndrome in coronavirus disease 2019: a narrative review [J]. *J Intern Med*, 2021, **289**(2): 147-161.

[21] Rizk JG, Kalantar-Zadeh K, Mehra MR, *et al*. Pharmaco-immunomodulatory therapy in COVID-19 [J]. *Drugs*, 2020, **80**(13): 1267-1292.

[22] Azevedo BC, Morel LJF, Carmona F, *et al*. Aqueous extracts from *Uncaria tomentosa* (Willd. ex Schult.) DC. reduce bronchial hyperresponsiveness and inflammation in a murine model of asthma [J]. *J Ethnopharmacol*, 2018, **218**: 76-89.

[23] Cheng RZ, Zhang CY, Li Y, *et al*. Study on chemical constituents of "decocted first and defoamed" of *Ephedra herba* by UPLC-DAD-TOF/MS and HPLC-UV [J]. *Chin Tradit Herb Drugs*, 2018, **49**(8): 1919-1923.

[24] Li, HY, Su D, Bu AX, *et al*. Chemical constituent changes in four processing procedures of herbal ephedra based on UPLC-Q TOF MS^{E} and mirror image contrast analysis [J]. *J Chin Mass Spectrom Society*, 2017, **38**(6): 630-639.

[25] Sun Q, Cao H, Zhou Y, *et al*. Qualitative and quantitative analysis of the chemical constituents in Mahuang-Fuzi-Xixin decoction based on high performance liquid chromatography combined with time-of-flight mass spectrometry and triple quadrupole mass spectrometers [J]. *Biomed Chromatogr*, 2016, **30**(11): 1820-1834.

[26] Zhang J, Xu XJ, Xu W, *et al*. Rapid Characterization and identification of flavonoids in Radix Astragali by ultra-high-pressure liquid chromatography coupled with linear ion trap-orbitrap mass spectrometry [J]. *J Chromatogr Sci*, 2015, **53**(6): 945-952.

[27] Li CY, Song HT, Liu SJ, *et al*. Systematic screening and characterization of astragalosides in an oral solution of Radix Astragali by liquid chromatography with quadrupole time-of-flight mass spectrometry and Peakview software [J]. *J Sep Sci*, 2016, **39**(6): 1099-1109.

[28] Shi HS, Bi XF, Shi XH. Analysis on the chemical consitituents of flavones and saponin in the root and the stem leaf off astragalus membranaceus with ultra-high performance liquid chromatography coupled with hybrid quadrupole-orbitrap mass spectrometry [J]. *World J Integrat Tradit Western Med*, 2018, **13**(3): 357-361.

[29] Yu H, Hu Q, Sun J, *et al*. Comprehensive screening of multi-conponents in huangqi injection by ultra-performance liquid chromatography coupled with quadrupole-time-of-flight mass sepctrometry [J]. *World Chin Med*, 2019, **14**(4): 809-817.

[30] Wang L, Yuan K, Yu WW, *et al*. Evaluation and discrimination of Cortex Magnoliae officinalis produced in Zhejiang Province (Wen-Hou-Po) by UPLC-DAD-TOF-MS fingerprint [J]. *Nat Prod Commun*, 2010, **5**(10): 1631-1638.

[31] Zhao H, Yan Y, Wang CC, *et al*. Comparison of chemical constituents in *Magnoliae officinalis* Cortex processed by "sweating" and "non sweating" based on ultra fast liquid chromatography-triple quadrupole-time of flight mass spectrometry and gas chromatography-triple quadrupole mass spectrometry combined with multivariate statistical analysis [J]. *Nat Prod Commun.*, 2018, **13**(8): 987-991.

[32] Yan R, Wang W, Guo J, *et al*. Studies on the alkaloids of the bark of Magnolia officinalis: isolation and on-line analysis by HPLC-ESI-MS(n) [J]. *Molecules*, 2013, **18**(7): 7739-7750.

[33] Guo K, Tong C, Fu Q, *et al*. Identification of minor lignans, alkaloids, and phenylpropanoid glycosides in *Magnolia officinalis* by HPLCDADQTOF-MS/MS [J]. *J Pharm Biomed Anal*, 2019, **170**: 153-160.

[34] Xue Z, Lai C, Kang L, *et al*. Profiling and isomer recognition of phenylethanoid glycosides from *Magnolia officinalis* based on diagnostic/holistic fragment ions analysis coupled with chemometrics [J]. *J Chromatogr A*, 2020, **1611**: 460583.

[35] Liu W, Ge GB, Wang YL, *et al*. Chemical consituent and tissue distribution study of qingfei paidu decoction in mice using UHPLC-Q-Orbitrap HRMS [J]. *Chin Tradit Herb Drugs*, 2020, **51**(8): 2035-2045.
[36] Wang YQ, Li S, Jiang X. On-line determination of antioxidant active ingredients of rhei radix et rhizama by HPLC-ABTS-DAD-Q-TOF/MS [J]. *Chin J Hosp Pharm*, 2019, **39**(11): 1149-1152.
[37] Yan Y, Zhang Q, Feng F. HPLC-TOF-MS and HPLC-MS/MS combined with multivariate analysis for the characterization and discrimination of phenolic profiles in nonfumigated and sulfur-fumigated rhubarb [J]. *J Sep Sci*, 2016, **39**(14): 2667-2677.
[38] Liang Z, Sham T, Yang G, *et al*. Profiling of secondary metabolites in tissues from *Rheum palmatum* L. using laser microdissection and liquid chromatography mass spectrometry [J]. *Anal Bioanal Chem*, 2013, **405**(12): 4199-4212.
[39] Han J, Ye M, Xu M, *et al*. Comparison of phenolic compounds of rhubarbs in the section *deserticola* with *Rheum palmatum* by HPLC-DAD-ESI-MS_n [J]. *Planta Med*, 2008, **74**(8): 873-879.
[40] Rahman MJ, Costa de Camargo A, Shahidi F. Phenolic profiles and antioxidant activity of defatted camelina and sophia seeds [J]. *Food Chem*, 2018, **240**: 917-925.
[41] Meng Z, Li W. Analysis of the constituents in *Semen descurainiae* by UPLC/Q-TOF-MS/MS [J]. *J Chin Pharm Sci*, 2015, **24**(5): 303-309.
[42] Li SL, Song JZ, Choi FF, *et al*. Chemical profiling of Radix Paeoniae evaluated by ultra-performance liquid chromatography/photo-diode-array/quadrupole time-of-flight mass spectrometry [J]. *J Pharm Biomed Anal*, 2009, **49**(2): 253-266.
[43] Liang J, Xu F, Zhang YZ, *et al*. The profiling and identification of the absorbed constituents and metabolites of Paeoniae Radix Rubra decoction in rat plasma and urine by the HPLC-DAD-ESI-IT-TOF-MS(n) technique: a novel strategy for the systematic screening and identification of absorbed constituents and metabolites from traditional Chinese medicines [J]. *J Pharm Biomed Anal*, 2013, **83**: 108-121.
[44] Liu EH, Qi LW, Li B, *et al*. High-speed separation and characterization of major constituents in Radix Paeoniae Rubra by fast high-performance liquid chromatography coupled with diode-array detection and time-of-flight mass spectrometry [J]. *Rapid Commun Mass Spectrom*, 2009, **23**(1): 119-130.
[45] Lian HY, Xu WYJ, Lian QD, *et al*. Chemical comparison between decoctions of Radix Paeoniae Rubra and Radix Paeoniae Alba by UPLC-QTOF MS [J]. *J Chin Mass Spectrom Society*, 2014, **35**(03): 269-278.
[46] Zhou HL, Xu SJ, L ZR, *et al*. Analysis of chemical constituents of *Radix Paeoniae alba* and *Radix Paeoniae Alba* by HPLC-TOF/MS [J]. *J Chin Med Mater*, 2018, **41**(7): 1637-1640.
[47] Liu J, Chen L, Fan CR, *et al*. Qualitative and quantitative analysis of major constituents of Paeoniae Radix Alba and Paeoniae Radix Rubra by HPLC-DAD-Q-TOF-MS / MS [J]. *China J Chin Mater Med*, 2015, **40**(9): 1762-1770.
[48] An JH, Yuk HJ, Kim DY, *et al*. Evaluation of phytochemicals in *Agastache rugosa* (Fisch. & C. A. Mey.) Kuntze at different growth stages by UPLC-QTof-MS [J]. *Ind Crops Prod*, 2018, **112**: 608-616.
[49] Desta KT, Kim GS, Kim YH *et al*. The polyphenolic profiles and antioxidant effects of *Agastache rugosa* Kuntze (Banga) flower, leaf, stem and root [J]. *Biomed Chromatogr*, 2016, **30**(2): 225-231.
[50] Anand S, Deighton M, Livanos G, *et al*. Antimicrobial activity of *Agastache* honey and characterization of its bioactive compounds in comparison with important commercial honeys [J]. *Front. Microbiol*, 2019, **10**: 263.
[51] Bielecka M, Zielińska S, Pencakowski B, *et al*. Age-related variation of polyphenol content and expression of phenylpropanoid biosynthetic genes in *Agastache rugosa* [J]. *Ind Crops Prod*, 2019, **141**: 111743.
[52] Zielińska S, Kolniak-Ostek J, Dziadas M, *et al*. Characterization of polyphenols in *Agastache* rugosa leaves and inflorescences by UPLC-qTOF-MS following FCPC separation [J]. *J Liq Chromatogr Relat Technol*, 2016, **39**(4): 209-219.
[53] Zhang Y, Bo C, Fan Y, *et al*. Qualitative and quantitative determination of *Atractylodes* rhizome using ultra-performance liquid chromatography coupled with linear ion trap-Orbitrap mass spectrometry with data-dependent processing [J]. *Biomed Chromatogr*, 2018, **33**(3): e4443.
[54] Li ZJ, Wan HY, Gu LL, *et al*. Extraction and LC-MS/MS analysis of the polyphenols from *Amomum tsaoko* [J]. *Sci Technol Food Industry*, 2017, **38**(8): 294-299.
[55] Lee JY, Park NH, Lee W, *et al*. Comprehensive chemical profiling of *Pinellia species* tuber and processed *Pinellia* tuber by gas chromatography-mass spectrometry and liquid chromatography-atmospheric pressure chemical ionization-tandem mass spectrometry [J]. *J Chromatogr A*, 2016, **1471**: 164-177.
[56] Zhai XY, Zhang L, Li BT, *et al*. Chemical Components in Pinelliae Rhizoma by UPLC-Q-TOF-MS/MS [J]. *Chin J Exp Tradit Med*, 2019, **25**(7): 173-183.
[57] Wu D, Yang XO. TH17 responses in cytokine storm of COVID-19: an emerging target of JAK2 inhibitor Fedratinib [J]. *J Microbiol Immunol Infect*, 2020, **53**(3): 368-370.
[58] Hotez PJ, Bottazzi ME, Corry DB. The potential role of Th17 immune responses in coronavirus immunopathology and vaccine-induced immune enhancement [J]. *Microbes Infect*, 2020, **22**(4-5): 165-167.

Cite this article as: WEI Wen-Long, WU Shi-Fei, LI Hao-Jv, LI Zhen-Wei, QU Hua, YAO Chang-Liang, ZHANG Jian-Qing, LI Jia-Yuan, WU Wan-Ying, GUO De-An. Chemical profiling of Huashi Baidu prescription, an effective anti-COVID-19 TCM formula, by UPLC-Q-TOF/MS [J]. *Chin J Nat Med*, 2021, **19**(6): 473-480.